Reactions between Iron(III) and Catechol (*o*-Dihydroxybenzene). Part II.[1] Equilibria and Kinetics of the Redox Reaction in Aqueous Acid Solution

By **Edoardo Mentasti, Ezio Pelizzetti,** and **Guido Saini,*** Istituto di Chimica Analitica, Università di Torino, Italy

The redox reaction between iron(III) and catechol (H_2cat) has been investigated at 25·0 °C and $1·0 > [H^+] \geqslant 0·1$M with the stopped-flow technique. The overall reaction (i) (qno = *o*-quinone) is limited by the reverse reaction

$$2Fe^{3+} + H_2cat \rightleftharpoons 2Fe^{2+} + qno + 2H^+ \quad (i)$$

and the equilibrium constant, obtained from spectrophotometric data, $K_{eq} = (2·2 \pm 0·1) \times 10^{-2}$ mol^2 l^{-2}; ε(qno) = $(1·46 \pm 0·07) \times 10^3$ l mol^{-1} cm^{-1} at 390 nm. The mechanism proposed involves intermediate semiquinone radical (Hcat·) formation as the rate-determining step; Hcat· is then oxidized to *o*-quinone, according to steps (ii) and (iii). The quantities k_1' and k_2'/k_3' vary with hydrogen-ion concentration according to $k_1' = k_1/[H^+]$

$$Fe^{3+} + H_2cat \underset{k_2'}{\overset{k_1'}{\rightleftharpoons}} Fe^{2+} + Hcat\cdot + H^+ \quad (ii)$$

$$Fe^{3+} + Hcat\cdot \underset{k_4}{\overset{k_3'}{\rightleftharpoons}} Fe^{2+} + qno + H^+ \quad (iii)$$

and $k_2'/k_3' = k_2[H^+]/k_3$, where $k_1 = 0·19 \pm 0·01$ s^{-1}, $k_2/k_3 = 0·88 \pm 0·08$ l mol^{-1}, and $k_4 = 10·8 \pm 1·0$ l mol^{-1} s^{-1} (independent of $[H^+]$). A comparison between kinetic and equilibrium data showed satisfactory agreement. The hydrogen-ion dependence of the reaction rates indicates that one of the reactants is deprotonated and alternative paths for reaction are discussed.

In Part I of this series it was shown that, in aqueous acidic media, catechol (H_2cat) reacts with iron(III) to form the complex $[Fe(cat)]^+$; this reaction is followed by oxidation of catechol to *o*-quinone (qno). Whereas the kinetics and equilibrium of formation of the complex was the subject of Part I, the present paper concerns the kinetics and equilibrium of the redox reaction.

Previous work on the kinetics of oxidation of diphenols concerned mainly quinol and inorganic oxidizing agents [Fe^{III},[2] I^{VII},[3] Mn^{III},[4,5] Ce^{IV},[6] Co^{III},[7] and Cr^{VI} (ref. 8)]. It has been found that the rate-determining step is semiquinone radical formation (corresponding to the first electron removal) when one-electron oxidizing agents are used, whereas oxidation with multi-electron oxidants, such as Cr^{VI}, takes place in a single step corresponding to direct formation of *p*-quinone. The only kinetic investigation on the oxidation of catechol was made with periodate ion [9] and the reaction was found to occur in a single step, as with quinol. Therefore it seemed of interest to investigate the oxidation of catechol with one-electron oxidants, such as iron(III), in order to ascertain if redox reaction follows the same mechanism both for quinol and for catechol. The kinetic experiments were made with an excess of catechol over the concentration of iron(III).

EXPERIMENTAL

Solutions of perchloric acid, sodium perchlorate (all the experimental measurements were performed at ionic strength 1·0M), catechol, and iron(III) perchlorate were prepared as described in Part I.[1] An iron(II) perchlorate solution was prepared by dissolving analytical grade iron wire (C.Erba ACS) in a known excess of aqueous perchloric acid (C.Erba RP). Purified nitrogen was bubbled through the mixture, and the filtered solution was titrated with standard potassium permanganate; the free hydrogen-ion concentration was calculated from the total perchloric acid and iron(II) concentrations.

The experiments were made with a stopped-flow spectrophotometer (Durrum–Gibson). A Teflon–quartz cell was used with a path length of 1·65 cm. All measurements were made at 25·0 ± 0·1 °C.

RESULTS AND DISCUSSION

Two solutions containing iron(III) and catechol respectively, adjusted to the same hydrogen-ion concentration (in the range $1·0 > [H^+] \geqslant 0·1$M) with perchloric acid, and to the same ionic strength, were mixed in the stopped-flow apparatus. After the start of the redox reaction the solution showed an absorption maximum at 390 nm. The absorbance at this wavelength increased with time. This maximum was assumed to be due to *o*-quinone, the oxidation product of catechol.[1] In the hydrogen-ion concentration range investigated the conditional formation constant of the iron(III)–catechol complex is very small so that this intermediate does not contribute significantly to the absorbance at 390 nm; also the absorbances of iron(III) or its hydrolysed species (the total concentration, $c_{Fe^{3+}}$, ranging from 4·0 to

[1] Part I, E. Mentasti and E. Pelizzetti, preceding paper.
[2] J. H. Baxendale, H. R. Hardy, and L. H. Sutcliffe, *Trans. Faraday Soc.*, 1951, **47**, 963.
[3] E. T. Kaiser and S. W. Weidman, *J. Amer. Chem. Soc.*, 1964, **86**, 4354.
[4] C. F. Wells and L. V. Kuritsyn, *J. Chem. Soc.* (*A*), 1970, 676.
[5] G. Davies and K. Kustin, *Trans. Faraday Soc.*, 1969, **65**, 1630.
[6] C. F. Wells and L. V. Kuritsyn, *J. Chem. Soc.* (*A*), 1969, 2575.
[7] C. F. Wells and L. V. Kuritsyn, *J. Chem. Soc.* (*A*), 1969, 2930.
[8] J. C. Sullivan and J. E. French, *J. Amer. Chem. Soc.*, 1965, **87**, 5380.
[9] W. Weidman and E. T. Kaiser, *J. Amer. Chem. Soc.*, 1966, **88**, 5820.

$6{\cdot}0 \times 10^{-4}$M), catechol (total concentration, c_{H_2cat}, from $1{\cdot}0$ to $4{\cdot}0 \times 10^{-2}$M), or iron(II) (total concentration, $c_{Fe^{2+}}$, from $1{\cdot}0$ to $6{\cdot}0 \times 10^{-3}$M) are negligible at this wavelength.

Equilibrium Data.—The closeness of the standard potentials [10] of the redox couples qno–H_2cat (qno = *o*-quinone and H_2cat = catechol) and Fe^{3+}–Fe^{2+} suggests that the overall redox reaction (1) does not go to completion, but is limited by the reverse reaction. Preliminary

$$2Fe^{3+}(aq) + H_2cat(aq) \rightleftharpoons 2Fe^{2+}(aq) + qno(aq) + 2H^+ \quad (1)$$

experiments showed that, by mixing a solution of catechol with solutions of iron(III) containing increasing amounts of iron(II), the concentration of *o*-quinone at equilibrium decreased. Further experiments performed by using vanadium(V) as oxidant showed that in this case *o*-quinone formation is increased compared to the case of iron(III), as a consequence of the higher standard potential of the V^{5+}–V^{4+} couple.[11]

As a result of these findings, an evaluation of the equilibrium constant, K_{eq}, of reaction (1) was made.

$$K_{eq} = K_{eq}'[H^+]^2 \quad (2)$$

This was undertaken by measuring, with the stopped-flow spectrophotometer, the absorbance at 390 nm due to

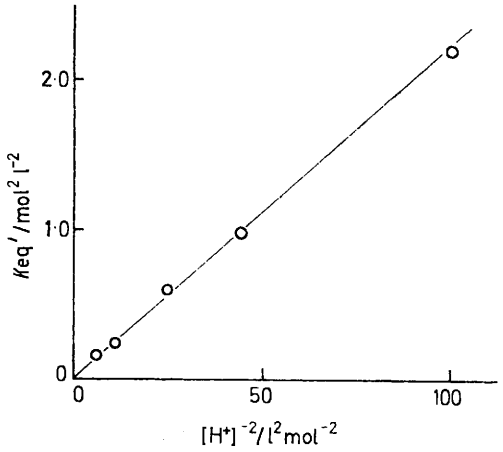

FIGURE 1 Hydrogen-ion dependence of K_{eq}'

o-quinone after equilibrium (1) had been attained and before the further slow reactions of coupling and polymerization of *o*-quinone [12] could take place, with subsequent separation of slightly soluble products. By working with an excess of catechol ($[H_2cat] \simeq c_{H_2cat}$), equation (2) can be rewritten as (3) [A = absorbance, l = path length, ε(qno) = absorption coefficient of qno at 390 nm].

$$K_{eq}' = \frac{(c_{Fe^{3+}} + 2[qno])^2[qno]}{(c_{Fe^{3+}} - 2[qno])^2 c_{H_2cat}} \quad (3)$$

where

$$[qno] = \frac{A}{l\varepsilon(qno)}$$

The best set of K_{eq}' and ε(qno) values was computed from experimental data (Table 1) at each $[H^+]$ value investigated. In Figure 1 average values of K_{eq}' are plotted against $[H^+]^{-2}$, according to equation (2). Calculated values of K_{eq} and ε(qno) are respectively $(2{\cdot}2 \pm 0{\cdot}1) \times 10^{-2}$ mol^2 l^{-2} and $(1{\cdot}46 \pm 0{\cdot}07) \times 10^3$ l mol^{-1} cm^{-1}. The latter value agrees with data concerning oxidation experiments of catechol with other oxidizing agents,[13] and can be compared with the value of $1{\cdot}8 \times 10^3$ l mol^{-1} cm^{-1} given in the literature.[14]

TABLE 1

Experimental data for the determination of the equilibrium constant K_{eq} and the absorption coefficient of *o*-quinone: $c_{H_2cat} = 2{\cdot}0 \times 10^{-2}$ and $c_{Fe^{3+}} = 6{\cdot}0 \times 10^{-4}$ mol l^{-1}

$[H^+]$ / mol l^{-1}	$10^3 c_{Fe^{3+}}$ / mol l^{-1}	A(390 nm)	K_{eq}' / mol^2 l^{-2}	$10^{-3}\varepsilon$(qno)l / l mol^{-1}
0·10	1·0	0·615	2·27	
	2·0	0·541	2·24	
	3·0	0·470	2·10	
	4·0	0·417	2·18	
	5·0	0·365	2·13	
			Av. 2·18 ± 0·09	2·50
0·15	1·0	0·523	0·97	
	2·0	0·428	0·92	
	3·0	0·360	0·97	
	4·0	0·301	0·98	
	5·0	0·258	1·03	
			Av. 0·97 ± 0·06	2·35
0·20	1·0	0·485	0·52	
	2·0	0·385	0·55	
	3·0	0·319	0·63	
	4·0	0·260	0·65	
	5·0	0·207	0·63	
			Av. 0·60 ± 0·05	2·40
0·30	1·0	0·398	0·20	
	2·0	0·280	0·22	
	3·0	0·207	0·24	
	4·0	0·146	0·23	
	5·0	0·114	0·24	
			Av. 0·23 ± 0·03	2·40
0·40	1·0	0·340	0·12	
	2·0	0·213	0·12	
	3·0	0·160	0·15	
			Av. 0·13 ± 0·02	2·40

Kinetics.—Assuming that the mechanism suggested for oxidation of quinol with one-electron oxidizing agents can be applied to the present reaction, steps (4) and (5) must be considered in equilibrium (1). Reaction

$$Fe^{3+}(aq) + H_2cat(aq) \underset{k_2}{\overset{k_1}{\rightleftharpoons}} Fe^{2+}(aq) + Hcat^{\cdot}(aq) + H^+(aq) \quad (4)$$

$$Fe^{3+}(aq) + Hcat^{\cdot}(aq) \underset{k_4}{\overset{k_3}{\rightleftharpoons}} Fe^{2+}(aq) + qno + H^+(aq) \quad (5)$$

[10] L. Jenny, *Helv. Chim. Acta*, 1949, **32**, 315.
[11] L. Meites, 'Handbook of Analytical Chemistry,' McGraw-Hill, London, 1965.
[12] H. Musso, 'Oxidative Coupling of Phenols,' eds. W. I, Taylor and A. R. Battersby, M. Dekker Inc., New York, 1967. ch. 1.
[13] E. Pelizzetti, E. Mentasti, and G. Saini, unpublished work.
[14] H. S. Mason, *J. Biol. Chem.*, 1949, **181**, 803.

(4) may be viewed as an overall reaction involving as intermediate steps outer-sphere complex formation of iron(III) (in its free or hydrolysed form) with catechol or a further step yielding an inner-sphere complex with partial or complete deprotonation of catechol. Assuming all these steps are fast compared to the oxidation step to semiquinone (see Part I), all these reactions can be considered to be at equilibrium during the redox reaction.

By carrying out kinetic experiments with an excess of H_2cat and H^+, so that $[H_2cat]$ and $[H^+]$ can be assumed constant during the reaction, equation (6), from (4) and (5), can be written, where k_1', k_2', k_3', and k_4' include

$$d[Hcat^\cdot]/dt = k_1'[Fe^{3+}]c_{H_2cat} - k_2'[Fe^{2+}][Hcat^\cdot] - k_3'[Fe^{3+}][Hcat^\cdot] + k_4'[Fe^{2+}][qno] \quad (6)$$

$[H^+]^n$ and n is the reaction order with respect to H^+. During the early part of the reaction [corresponding to the reduction of less than 10% of the total iron(III)], the approximation $[Fe^{3+}]$ = constant (in excess over semiquinone) can be made so that equation (7) is obtained, where $\bar{c}_{Fe^{3+}}$ is the average concentration of iron(III).

$$d[Hcat^\cdot]/dt = k_1'[Fe^{3+}]c_{H_2cat} - k_2'[Fe^{2+}][Hcat^\cdot] - k_3'\bar{c}_{Fe^{3+}}[Hcat^\cdot] + k_4'[Fe^{2+}][qno] \quad (7)$$

Assuming steady-state conditions for $Hcat^\cdot$, equation (8) can be obtained and the rate of formation of qno,

$$[Hcat^\cdot] = \frac{k_1'[Fe^{3+}]c_{H_2cat} + k_4'[Fe^{2+}][qno]}{k_2'[Fe^{2+}] + k_3'\bar{c}_{Fe^{3+}}} \quad (8)$$

according to reaction (5), is given by (9). Because the

$$d[qno]/dt = k_3'\bar{c}_{Fe^{3+}}[Hcat^\cdot] - k_4'[qno][Fe^{2+}] \quad (9)$$

initial rate of formation of qno is not significantly affected by the terms containing k_4' [the contribution of the reverse of reaction (5)], equation (10) holds, or, in integrated form, (11). By plotting the left-hand side

$$\frac{d[qno]}{dt} = k_3'\bar{c}_{Fe^{3+}}\frac{k_1'c_{H_2cat}(c_{Fe^{3+}} - 2[qno])}{k_2'(c_{Fe^{3+}} + 2[qno]) + k_3'\bar{c}_{Fe^{3+}}} \quad (10)$$

of equation (11) as a function of time, t, a straight line was obtained with gradient, to a first approximation, given by (12). Equation (12) can be further rearranged

$$\ln\frac{c_{Fe^{3+}}}{c_{Fe^{3+}} - 2[qno]} = \frac{2k_1'c_{H_2cat}t}{1 + (c_{Fe^{3+}} + c_{Fe^{2+}})k_2'/k_3'\bar{c}_{Fe^{3+}}} + \frac{2[qno]}{k_3'\bar{c}_{Fe^{3+}}/k_2' + c_{Fe^{3+}} + c_{Fe^{2+}}} \quad (11)$$

$$\alpha = \frac{2k_1'c_{H_2cat}}{1 + (c_{Fe^{3+}} + c_{Fe^{2+}})k_2'/k_3'\bar{c}_{Fe^{3+}}} \quad (12)$$

as (13). This equation permits evaluation, to a first

$$\frac{1}{\alpha} = \frac{1}{2k_1'c_{H_2cat}} + \frac{k_2'}{2k_1'k_3'c_{H_2cat}\bar{c}_{Fe^{3+}}}(c_{Fe^{3+}} + c_{Fe^{2+}}) \quad (13)$$

approximation, of k_1' and k_2'/k_3': by successive approximations [in order to account for the second term on the right-hand side of equation (11)], values of α can be evaluated.

In Figure 2 the initial data of some runs made at $[H^+] = 0{\cdot}20$M and constant c_{H_2cat} at $c_{Fe^{3+}}$ and with

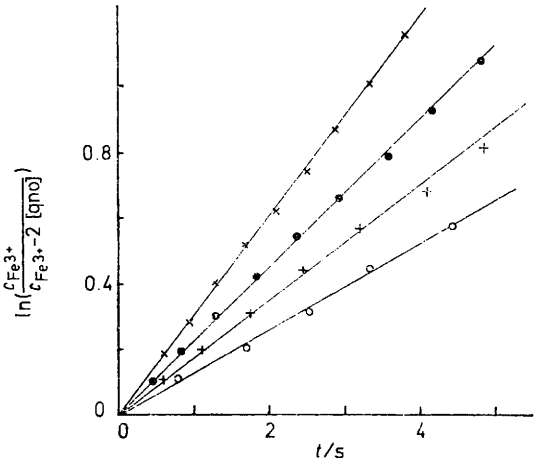

FIGURE 2 Plot of some experimental runs according to equation (11), after the third approximation: $[H^+] = 0{\cdot}20$; $c_{H_2cat} = 2{\cdot}0 \times 10^{-2}$; $c_{Fe^{3+}} = 6{\cdot}0 \times 10^{-4}$; $c_{Fe^{2+}} = 0$ (×), $2{\cdot}0 \times 10^{-3}$ (●), $4{\cdot}0 \times 10^{-3}$ (+), and $6{\cdot}0 \times 10^{-3}$M (○)

different iron(II) concentrations are plotted as $\ln[c_{Fe^{3+}}/(c_{Fe^{3+}} - 2[qno])]$ against time, after the third approximation. The gradients of the plots (*i.e.* α) decrease with increasing $c_{Fe^{3+}}$ in agreement with (12). Values of $1/\alpha$ obtained from the kinetic runs at $[H^+] = 0{\cdot}20$M are plotted in Figure 3, according to equation (13). They

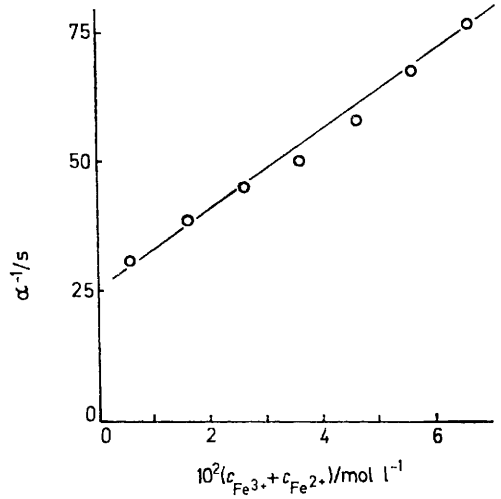

FIGURE 3 Plot of $1/\alpha$ against $(c_{Fe^{3+}} + c_{Fe^{2+}})$ according to equation (13) for kinetic runs at $[H^+] = 0{\cdot}20$, $c_{H_2cat} = 2{\cdot}0 \times 10^{-2}$, and $c_{Fe^{3+}} = 6{\cdot}0 \times 10^{-4}$M

lie reasonably well on a straight line, as expected. From this plot, values of k_1' and k_2'/k_3' were evaluated. The same kind of agreement of the experimental data with the theoretical treatment was found by working at different hydrogen-ion concentrations. Figure 4 shows

the plots of some typical runs concerning kinetic experiments where no iron(II) was added. In accordance with the theoretical treatment, the initial points fall on

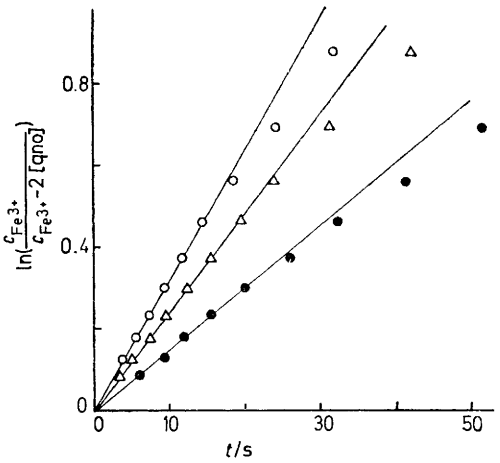

FIGURE 4 Plot of experimental data according to equation (11) at $[H^+] = 0.20$, $c_{Fe^{3+}} = 0$, and $c_{Fe^{3+}} = 4.0 \times 10^{-4}$M. c_{H_2cat} $= 1.0 \times 10^{-2}$ (●), 1.5×10^{-2} (△), and 2.0×10^{-2}M (○)

straight lines but deviate more and more as the reaction progresses, because both the assumptions of constant $[Fe^{3+}]$ and limited contribution from the reverse of

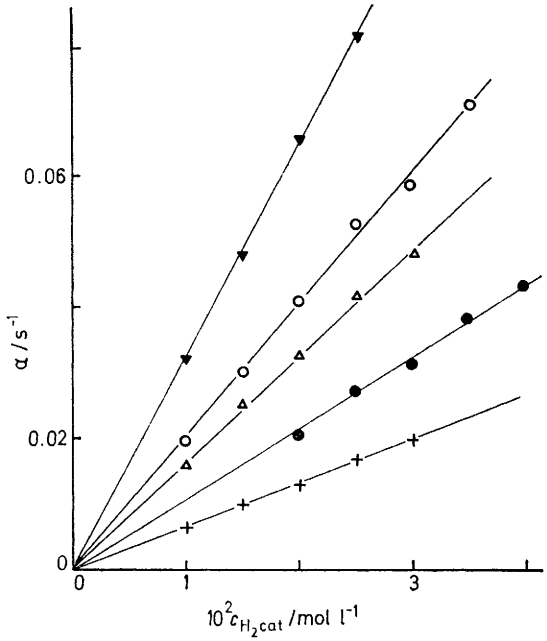

FIGURE 5 Plot of α [according to equation (12)] against c_{H_2cat} for the kinetic runs with $c_{Fe^{3+}} = 0$. $[H^+] = 0.10$ (▼), 0.15 (○), 0.20 (△), 0.30 (●), and 0.40M (+)

reaction (5) [see equations (7) and (10)] are no longer valid.

In Figure 5 initial gradients α of curves given in Figure 4 (and of other runs not included) are plotted as a function of c_{H_2cat}, the concentration of catechol. Each curve corresponds to a different hydrogen-ion concentration. The linearity shows that α is directly proportional to c_{H_2cat} in agreement with (12). Experimental data,

TABLE 2

Experimental data for the evaluation of k_1' and k_2'/k_3': $c_{H_2cat} = 2.0 \times 10^{-2}$ and $c_{Fe^{3+}} = 6.0 \times 10^{-4}$ mol l⁻¹

$[H^+]$ / mol l⁻¹	$10^3 c_{Fe^{3+}}$ / mol l⁻¹	$10^3\alpha$ / s⁻¹	k_1' / l mol⁻¹ s⁻¹	k_2'/k_3'
0·10	0·0	64·4		
	1·0	59·8		
	2·0	54·1		
	3·0	49·2		
	4·0	46·5		
	5·0	41·9	1·85	0·076
0·15	0·0	42·3		
	1·0	36·1		
	2·0	33·1		
	3·0	29·2		
	4·0	27·1		
	5·0	24·6		
	6·0	22·5	1·20	0·098
0·20	0·0	31·7		
	1·0	25·5		
	2·0	22·1		
	3·0	19·9		
	4·0	17·2		
	5·0	14·7		
	6·0	13·1	1·00	0·169
0·30	0·0	20·4		
	1·0	13·9		
	2·0	10·9		
	3·0	8·7		
	4·0	7·2		
	5·0	6·3		
	6·0	5·6	0·62	0·283
0·40	0·0	13·7		
	1·0	9·5		
	2·0	7·5		
	3·0	6·3	0·46	0·325

concerning the valuation of k_1' and k_2'/k_3', are collected in Table 2. Figure 6 shows that k_1' is a linear function

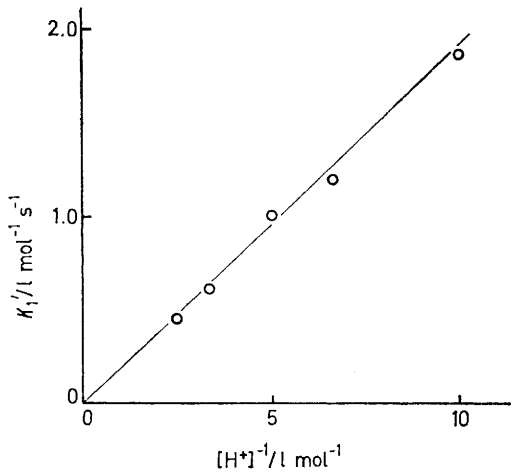

FIGURE 6 Hydrogen-ion dependence of k_1'

of $[H^+]^{-1}$, and Figure 7 shows the dependence of k_2'/k_3' on $[H^+]$, so that $k_1' = k_1/[H^+]$ and $k_2'/k_3' = k_2[H^+]/k_3$. The kinetic constants obtained are collected in Table 3.

In order to estimate k_4 by direct kinetic measurements, a solution of catechol was oxidized to *o*-quinone by mixing with a solution of vanadium(V) (slightly

less than theoretical amount required to oxidize all the catechol). The solution was then immediately mixed

TABLE 3

Rate constants found for the redox reaction of catechol with iron(III) at 25·0 °C and I = 1·0M

k_1/s^{-1}	0·19 ± 0·01
(k_2/k_3)/l mol^{-1}	0·88 ± 0·08
k_4/l mol^{-1} s^{-1}	10·8 ± 1·0

in the stopped-flow apparatus with a solution of iron(II) in excess, with $c_{Fe^{2+}}$ assumed constant during the reaction. The reagents were previously thermostatted

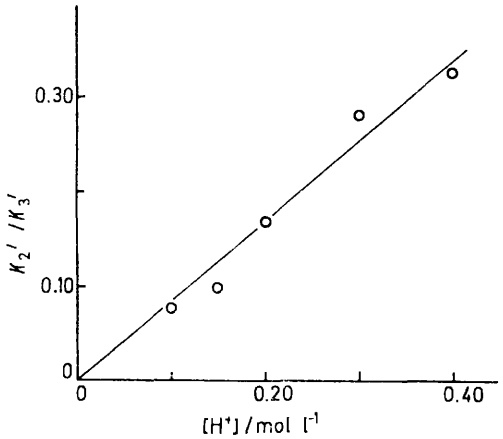

FIGURE 7 Hydrogen-ion dependence of k_2'/k_3'

and brought to ionic strength 1·0M and the desired hydrogen-ion concentration.

evaluated. The experimental conditions were $[qno]_0 = 1{\cdot}6 \times 10^{-4}$, $c_{Fe^{3+}} = 5{\cdot}0 \times 10^{-3}$, and $[H^+] = 0{\cdot}20$ and 0·40M and the kinetic data, according to equation (14), gave straight lines with zero intercept; from the gradients of these lines k_4' was estimated as 10·5 and 11·2 l mol^{-1} s^{-1} respectively at $[H^+] = 0{\cdot}20$ and 0·40M. It is noteworthy that the dependences of K_{eq}', k_1', and k_2'/k_3' on $[H^+]$ suggest that k_4' is independent of hydrogen-ion concentration; the two measurements at $[H^+] = 0{\cdot}20$ and 0·40M support this finding, so that $k_4' = k_4$. The same dependence on $[H^+]$ was observed for the corresponding rate constants in the redox reaction between quinol and iron(III).[2]

In order to test if the calculated kinetic constants are consistent with the equilibrium data, equation (2) can be rewritten as (16); K_{eq} was found to be $2{\cdot}2 \times 10^{-2}$ mol^2 l^{-2}, whereas the corresponding value from the

$$K_{eq} = k_1(k_3/k_2)(1/k_4) \qquad (16)$$

kinetic constants was $2{\cdot}0 \times 10^{-2}$ mol^2 l^{-2}. The agreement obtained by the two independent methods is satisfactory and supports the validity of the theoretical treatment.

Turning now to the reaction mechanism, the dependence on $[H^+]^{-1}$ of the forward reaction of equation (4) suggests a path in which one of the reagents is deprotonated. The alternative paths (17)—(19) leading to Hcat$^\bullet$ should be considered, where formulae in parentheses indicate outer-sphere complexes. Path (17) involves prior hydrolysis of Fe^{3+}(aq) and formation of an outer-sphere complex with undissociated catechol; this

$$Fe^{3+}(aq) \rightleftharpoons [FeOH]^{2+}(aq) + H^+(aq)$$

$$[FeOH]^{2+}(aq) + H_2cat(aq) \rightleftharpoons \{Fe(OH)(H_2cat)\}^{2+}(aq) \overset{a}{\rightleftharpoons} Fe^{2+}(aq) + Hcat^\bullet(aq) + H_2O \qquad (17)$$

$$\{Fe(OH)(H_2cat)\}^{2+}(aq) \overset{b}{\rightleftharpoons} [Fe(Hcat)]^{2+}(aq) + H_2O$$

$$Fe^{3+}(aq) + H_2cat(aq) \rightleftharpoons \{Fe(H_2cat)\}^{3+}(aq) \overset{-H^+}{\rightleftharpoons} [Fe(Hcat)]^{2+}(aq) \rightleftharpoons Fe^{2+}(aq) + Hcat^\bullet(aq) \qquad (18)$$

$$Fe^{3+}(aq) + H_2cat(aq) \rightleftharpoons \{Fe(H_2cat)\}^{3+}(aq) \overset{-2H^+}{\rightleftharpoons} [Fe(cat)]^{+}(aq) \overset{+H^+}{\rightleftharpoons} Fe^{2+}(aq) + Hcat^\bullet(aq) \qquad (19)$$

By applying the same kinetic treatment to reaction (4) under steady-state conditions for Hcat$^\bullet$ and by adopting the same approximations as above, equation (14), similar to (11), can be obtained, where $[qno]_0$ and

$$\ln\frac{[qno]_0}{[qno]} - \frac{2([qno]_0 - [qno])}{c_{Fe^{3+}}(k_2[H^+])/k_3 + [Fe^{3+}]_0 + 2[qno]_0} = \frac{k_4'c_{Fe^{3+}}t}{1 + ([Fe^{3+}]_0 + 2[qno]_0)k_3/k_2[H^+]c_{Fe^{3+}}} \qquad (14)$$

$[Fe^{3+}]_0$ are concentrations at zero time. By plotting the left-hand side of (14) (with the value of k_2/k_3 previously found) against t, a straight line was obtained with intercept zero and initial gradient [when no iron(III) was added] given by equation (15), from which k_4' can be

$$\beta = \frac{k_4'c_{Fe^{3+}}}{1 + (2[qno]_0k_3/k_2[H^+]c_{Fe^{3+}})} \qquad (15)$$

in turn can undergo the redox reaction either directly [path (*a*)], or after formation of the inner-sphere complex [path (*b*)]. Paths (18) and (19) assume that the redox reaction occurs through intermediate formation of an inner-sphere complex from Fe^{3+}(aq) and H_2cat; the inner-sphere complex is monodentate (*i.e.* monoprotonated) in the former case, and bidentate (*i.e.* deprotonated) in the latter. Paths (17)—(19), kinetically indistinguishable, agree with the observed dependence on $[H^+]^{-1}$.

In the oxidation of quinol by iron(III) (where similar kinetic behaviour was found to that in the present reaction) Baxendale and his co-workers [2] suggested that of the alternative paths [path (19) is, of course, excluded] the most probable is the redox reaction of Fe^{3+}(aq) with the monoprotonated form of quinol,

rather than the reaction of $[FeOH]^{2+}(aq)$ with undissociated quinol. Therefore the suggested mechanism corresponds to path (18) in the present case. The mechanism proposed by Wells and Kuritsyn, however, for quinol oxidation with various aquometal ions, suggests that the different dependences on $[H^+]$ found for cerium(IV) [6] (independent), vanadium(V) [15] (dependent on $[H^+]$), and manganese(III) [4] (dependent on $[H^+]^{-1}$) can be related to the hydrolysis or protonation capability of the metal ions. It seems therefore reasonable to assume that the present reaction goes essentially through path (17). Paths (18) and (19) might also contribute to the overall reaction, because of the ability of catechol to form a chelate complex with iron(III); this contribution however appears to be small due to the very limited complex formation in the $[H^+]$ range investigated.

We thank Consiglio Nazionale delle Ricerche (Rome) for support.

[3/551 *Received*, 15*th March*, 1973]

[15] C. F. Wells and L. V. Kuritsyn, *J. Chem. Soc.* (*A*), 1970, 1372.